



1       **Quasi 10-day wave modulation of equatorial ionization anomaly during the Southern**  
2                               **Hemisphere stratospheric warming of 2002**

3  
4 Xiaohua Mo<sup>1\*</sup>

5  
6 1, College of Science, Key Laboratory for Ionospheric Observation and Simulation, Guangxi University for  
7 Nationalities, Nanning, China

8  
9 Correspondence to: Xiaohua Mo, [moxiaohua9999@163.com](mailto:moxiaohua9999@163.com)

10

11 **Key Points:**

- 12 • Southern Hemisphere SSW effects on EIA in Asian sector
- 13 • Quasi 10-day periodic oscillation in EIA region modulated by planetary wave
- 14 • In-phase relationship of quasi 10-day oscillation between northern and southern EIA crests

15

16 **Abstract**

17       The present paper studies the perturbations in equatorial ionization anomaly (EIA) region during the  
18 Southern Hemisphere (SH) sudden stratospheric warming (SSW) of 2002, using the location of EIA crests  
19 derived from Global Positioning System (GPS) station observations and the Total Electron Content (TEC)  
20 obtained by International GNSS Service (IGS) global ionospheric TEC map (GIMs) in Asian sector. A  
21 strong quasi 10-day periodic oscillation is clearly identified in EIA region, and it has in-phase relationship  
22 between northern and southern EIA crests. An eastward phase progression of quasi 10-day wave is also  
23 seen in polar stratospheric temperature during this period, suggesting the enhanced quasi-10-day planetary  
24 wave associated with SSW produced oscillation in EIA region through modulating the equatorial fountain  
25 effect. Our results reveal some newer features of ionospheric variation that have not been reported during  
26 Northern Hemisphere (NH) SSWs.

27

28

29

30



31 **1. Introduction**

32 Sudden stratospheric warming (SSW) is large-scale meteorological process in the polar stratosphere  
33 which is characterized by rapid rise in temperatures and deceleration/reversal in the zonal mean flows  
34 (Scherhag, 1952). The primary driver of SSW is thought to be a rapid growth of quasi-stationary planetary  
35 wave interacting with zonal mean flow (Matsuno, 1971). Although the main processes of SSW occur in the  
36 middle atmosphere, its effects on the ionosphere have been observed in significant changes of equatorial  
37 electrojet (EEJ), vertical plasma drift, and equatorial ionization anomaly (EIA) (Vineeth et al., 2007; Chau  
38 et al., 2009; Goncharenko et al., 2010). These ionospheric variations mainly display similar semidiurnal  
39 pattern and 13- to 16-day wave signatures which have been associated with planetary wave, solar and lunar  
40 tide wave (Pedatella and Forbes, 2009; Goncharenko et al., 2010; Fejer et al., 2010; Park et al., 2012).  
41 Since planetary waves in the Southern Hemisphere (SH) generally have smaller amplitudes than in the  
42 Northern Hemisphere (NH) where orographic and thermal forcing is stronger (Andrews et al., 1987), major  
43 SSWs often occur in NH. Therefore, most studies about SSW effects on the ionosphere are during NH  
44 SSW period.

45 In August to September 2002, three minor SSWs and a major SSW appeared in SH (Varotsos 2002;  
46 Baldwin et al., 2003). There is sufficient evidence that a series of unusual atmospheric states occurred in  
47 this period, i.e., planetary wave scale quasi 10-day variation (Krüger et al., 2005; Palo et al., 2005),  
48 short-term semidiurnal tide variability with zonal wave number  $s=1$  (Chang et al., 2009) and the winds  
49 oscillation with  $\sim 14$ -days period (Andrew et al., 2004), are all linked to the extremely large planetary wave  
50 events. Although the atmospheric activity in connection with 2002 SH SSW has been well revealed in  
51 observations and numerical modeling, relatively little is known about the ionosphere effects of 2002 SH  
52 SSW. Recently, Olson et al. (2013) studied the equatorial electrodynamic perturbations in Peruvian sector  
53 during 2002 SH SSW and found enhanced quasi 2-day fluctuations and large amplitude multi-day  
54 perturbations in EEJ and vertical drifts. The researches of ionospheric behavior during SH SSW periods are  
55 useful for verifying the existing explanation about the origin of ionospheric perturbations during NH SSW  
56 periods and revealing some newer features of ionospheric variation, so further investigation of 2002 SH  
57 SSW effect on ionosphere with more ionospheric parameters is still warranted.

58 In the present study, we present the first observational evidence of quasi 10-day oscillation in EIA  
59 region during 2002 SH SSW which has not been reported during NH SSWs, based on the location of EIA  
60 crests derived from Global Positioning System (GPS) station observations and the Total Electron Content



61 (TEC) obtained by International GNSS Service (IGS) global ionospheric TEC map (GIMs) in Asian sector.

62

## 63 **2. Data and Methods**

64 The location of EIA crests derived from GPS observations are used to analyze the variation in EIA  
65 region during 2002 SH SSW from July 21, 2002 to October 18, 2002. The GPS stations are GUAN  
66 (23.19°N, 113.34°E, MLAT~12.52°N) and BAKO (6.49°S, 106.84°E, MLAT~17.18°S) which are near  
67 northern and southern EIA crest, respectively. Since the ionospheric vertical TEC usually reach the  
68 maximum at EIA crest, the location of EIA crest can be obtained by vertical TEC values at each  
69 ionospheric penetration point (IPP), which is the intersection of the line of sight and the ionospheric shell  
70 (assumed to be 400 km) (Mo et al., 2014). The relative accuracy of the TEC is 0.02 total electron content  
71 unit (1TECU= $10^{16}$  el m<sup>-2</sup>) (Hofmann-Wellenhof et al., 1992). The sample rate of these GPS stations were  
72 30s, so the resolution of the location of EIA crest is less than 25 km (Mo et al., 2017). Figures 1a and 1b  
73 show the daily average geomagnetic latitude (MLAT) of northern and southern EIA crests during 2002 SH  
74 SSW.

75 The TEC from GIMs are also used to analyze the variation in EIA region. The GIMs provides maps of  
76 TEC obtained from a global network of GPS receivers, which have temporal resolution of 2 hours and  
77 spatial resolution of 5° in longitude and 2.5° in latitude (Mannucci et al., 1998). The EIA crest usually  
78 reaches its maximum development near 14:00 LT (Huang et al., 1989; Yeh et al., 2001), so the daily  
79 average TEC obtained by GIMs at 12~14 LT, ±5°~±15°N MLAT, 100°~150°E every day in Asian sector  
80 are used to describe the variation in northern and southern EIA region, the results are shown in Figures 1c  
81 and 1d.

82 The polar stratospheric temperature (90°S, 10hPa) and zonal mean zonal winds (60°S, 10hPa)  
83 obtained from National Centers for Environment Prediction (NCEP) are used to examine the extent of the  
84 SSW, the results are shown in Figures 1e and 1f. The background of geomagnetic activity index (Kp) and  
85 solar flux index (F10.7) from the websites <http://spidr.ngdc.noaa.gov/> are depicted in Figures 1g and 1h.

## 86 **3. Results and Analysis**

87 It can be seen from Figures 1e and 1f that there were three obvious minor SH SSW events around day  
88 number 230-260 and a major SH SSW event around day number 263-288 (Olson et al., 2013). Figure 2  
89 shows the contour map of polar stratospheric temperature (80°S, 10hPa) obtained from NCEP from July 21,  
90 2002 to October 18, 2002. An eastward phase progression of quasi 10-day wave is clearly observed around



91 day number 210-270. With SABER temperature data, Palo et al. (2005) also observed similar disturbance  
92 and suggested it consists eastward-propagating quasi 10-day wave with zonal wave numbers  $s=1$   
93 superimposed upon a large stationary planetary wave with  $s=1$ .

94 Now we examine the impact of this quasi 10-day wave on EIA region. It should be noted the  
95 solar/magnetospheric forcing on ionosphere are strong due to 2002 SH SSW event occurring during solar  
96 maximum year. To exclude these long period fluctuations in EIA region associated with  
97 solar/magnetosphere forcing, the periods longer than 15 days in the MLAT location and TEC of EIA crest  
98 are removed. The residuals of these parameters from 15-day running mean are subjected to Lomb-Scargle  
99 (L-S) spectral analysis (Lomb, 1976; Scargle, 1982), and the results are shown in Figures 3a, 3b, 3c, and 3d.  
100 The horizontal dashed lines represent the 90% confidence level. It is evident that the MLAT location and  
101 TEC of EIA crest all exhibit significant quasi 10-day periodic component, which exceed or approach 90%  
102 confidence level, suggesting that the whole dynamical process in EIA region is modulated by quasi 10-day  
103 wave. Figures 3 e and 3f show the L-S spectral analysis of Kp and F10.7. It can be seen that spectral  
104 component of Kp also has quasi 10-day periodic component which will be related to solar wind high-speed  
105 streams (Lei et al., 2008). However, this quasi 10-day periodic component is too weak to identify in F10.7,  
106 indicating that variation in the solar flux cannot account for this quasi 10-day oscillation in EIA region.

107 To investigate the time evolutions of quasi 10-day periodic variation, the Morlet wavelet spectral  
108 analysis is applied to MLAT location and TEC of EIA crest, and Kp which exhibit quasi 10-day oscillation.  
109 The periods longer than 15 days in the MLAT location and TEC of EIA crest are removed before the  
110 wavelet spectra is generated, and the results are illustrated in Figures 4a, 4b, 4c, and 4d. The black solid  
111 contours in each panel indicate a significance level higher than 95%. The white line in each panel  
112 represents the cone of influence of the wavelet analysis. The color bar number is the power strength for  
113 each parameter. Obviously, the most predominant periodic component in the MLAT location and TEC of  
114 EIA crest are quasi 10-day period, which mainly appeared around day number 210-290, indicating quasi  
115 10-day oscillations in EIA region go through three minor SSWs and a major SSW period. The time  
116 evolution of the power in MLAT location and TEC of northern EIA crest match well those of southern EIA  
117 crest, respectively. In addition, we note both the MLAT location and the TEC of EIA crest show the quasi  
118 2-day oscillations during major SSW period (around day number 260-270), which are also found on  
119 equatorial ionospheric electric fields and currents at the same period (Olson et al., 2013). Figure 4e shows  
120 the wavelet spectral analysis of Kp index. It can be seen that quasi 10-day periodic component is nearly



121 absent in Kp around day number 230-290, suggesting that magnetic activity should not be the driving force  
122 for this quasi 10-day oscillation in EIA region.

123 In order to demonstrate the phase relationship of the quasi 10-day oscillations between northern and  
124 southern EIA crests, the band-pass filter is performed on the TEC and MLAT location of EIA crest. The  
125 absolute values of the MLAT location of EIA crest are used. The band-pass filter is centered at the period of  
126 10-day, with half-power points at 8-day and 12-day, and the results are shown in Figure 5. Note that quasi  
127 10-day oscillations of northern and southern EIA crests are in-phase, which are consistent with quasi  
128 16-day oscillations in northern and southern EIA crests during 2002-2003 NH SSW, suggesting quasi  
129 10-day oscillations of northern and southern EIA crests are caused by common physical processes, e.g.  
130 fountain effect (Mo et al., 2018).

131

#### 132 **4. Discussions**

133 In recent years a series of reports have focused on ionospheric perturbations during SSW event. The  
134 most predominant features in ionosphere associated with SSW event are semidiurnal pattern and 13- to  
135 16-day wave variations, which are attributed to nonlinear interaction of planetary wave, solar and lunar tide  
136 wave (Pedatella and Forbes, 2009; Goncharenko et al., 2010; Fejer et al., 2010; Park et al., 2012). As major  
137 SSW often occurs in NH, most studies about SSW effects on the ionosphere are during NH SSW period. In  
138 August to September 2002, the first major SSW was observed in SH. The NH and SH SSW occurred in  
139 Arctic and Antarctic winter, respectively, so the occurring time and location of SH SSW are opposite to  
140 those of NH SSW. The researches of ionospheric behavior during SH SSW periods are useful for testing  
141 the general rule of ionospheric perturbations during NH SSW periods. For example, Olson et al. (2013)  
142 demonstrated that multi-day ionospheric perturbations responding to 2002 SH SSW resemble those  
143 observed during NH SSWs and these ionospheric perturbations were associated with enhanced lunar tidal  
144 effects.

145 In the current study we present observations of quasi 10-day oscillation in EIA region during the 2002  
146 SH SSW that has not been reported during NH SSWs. This quasi 10-day oscillation is absent and weak in  
147 Kp and F10.7 index, indicating that the magnetic activity and solar flux cannot account for this quasi  
148 10-day oscillation in EIA region. Meanwhile, an unusual atmospheric state occurred in this period that the  
149 ozone hole over the Antarctic has a smaller size and splits into two separate holes (Varotsos 2002; Baldwin  
150 et al., 2003). This phenomenon is thought to be due to high temperatures the Antarctic, which was



151 contributed to by upward propagation of a planetary wave (Venkat Ratnam et al., 2004). Moreover, strong  
152 planetary wave scale quasi 10-day variation was observed in polar stratospheric temperature during this  
153 period, so the quasi 10-day oscillations in EIA region may be related to atmosphere perturbations linking  
154 the SSW in the Southern Hemisphere.

155 A series of studies had showed how the quasi 10-day planetary wave in stratosphere can penetrate  
156 into the ionosphere E region. Krüger et al. (2005) revealed the eastward-traveling waves with periods near  
157 10 days and their interaction with quasi-stationary planetary waves forced in the troposphere during 2002  
158 SH SSW event, supporting the observational and numerical evidence that the eastward traveling wave  
159 interacts with the stationary wave to produce a quasi-periodic amplitude modulation of the stationary waves  
160 (Hirota et al., 1990; Ushimaru and Tanaka, 1992). Palo et al. (2005) found an eastward-propagating quasi  
161 10-day wave with zonal wave numbers  $s=1$  and  $s=2$ , and a quasi-stationary planetary waves with  $s=1$   
162 extend from the lower stratosphere to the 100-120 km height region with little amplitude attenuation. While  
163 the quasi-stationary planetary wave is confined to the high latitude atmosphere and cannot directly  
164 propagate to equatorial ionosphere, the tides were introduced into planetary wave modulation mechanism.  
165 Eswaraiiah et al. (2018) reported that zonal diurnal and semidiurnal tide amplitudes in Antarctica  
166 mesosphere and lower thermosphere were enhanced around day number 230-290 during 2002 SH SSW,  
167 which coincides with the enhanced period of quasi 10-day oscillations in EIA region shown in Figure 4.  
168 Moreover, Chang et al. (2009) showed that the short-term variability of the  $s=1$  semidiurnal tide is strongly  
169 dependent upon the PW1 events (quasi-10-day wave) prior to the major warming during 2002 SH SSW,  
170 supporting the suggestion that the quasi-stationary planetary wave can influence migrating and  
171 nonmigrating solar tides globally (Liu et al., 2010; Pedatella and Forbes, 2010). So the interactions between  
172 quasi-10-day planetary wave and tide will modify the ionosphere E-region winds, which can produce  
173 E-region electric fields via the E-region dynamo process. The E-region electric fields map to F-region  
174 along the magnetic field lines and generate an eastward electric field (Goncharenko, 2010). At the magnetic  
175 equator, the eastward electric field with quasi 10-day periodic variation change electron density distribution  
176 in the low-latitude region via  $\vec{E} \times \vec{B}$  drift, and finally leads to quasi 10-day planetary waves characteristic  
177 variations in EIA region. The effects of planetary wave on the equatorial fountain effect have been revealed  
178 by the evidence that the vertical and latitudinal structures of the 6-day oscillation in the F region ionosphere  
179 peak on both sides of the equator in the EIA region (Gu et al., 2014). The synchronous 10-day oscillation  
180 between northern and southern EIA crest in our results are consistent with these observations.



181 In our prior studies, a 14- to 15-day wave during several NH SSW events is ascribed to lunar tide  
182 (Mo et al., 2018). So the source of quasi 10-day oscillations in EIA region during 2002 SH SSW is different  
183 from 14- to 15-day waves during NH SSW. Moreover, no obvious 14- to 15-day oscillation is found in EIA  
184 region during 2002 SH SSW, which may be that the equatorial lunar semidiurnal effects during  
185 September-October are weaker than that during January-February (Stening et al., 2011; Pedatella, 2014).  
186 Olson et al. (2013) also reported that the perturbations amplitude of EEJ and vertical drifts modulated by  
187 lunar semidiurnal tides during SH SSW are smaller than those during NH SSW.

188

## 189 **5. Conclusions**

190 Using the location and TEC of EIA crests derived from GPS station observations and GIMs, we found  
191 a quasi 10-day periodic variability in EIA region in Asian sector during the SH SSW of 2002. This quasi  
192 10-day oscillation is in-phase between northern and southern EIA crests. In the same time period, this quasi  
193 10-day oscillation is also seen in the polar stratospheric temperature, which is absent and weak in Kp and  
194 F10.7 index, respectively. Previous studies have shown that a strong quasi 10-day planetary wave with  
195 zonal wave numbers  $s=1$  extend from the lower stratosphere to mesosphere and lower thermosphere (Palo  
196 et al., 2005), so the quasi 10-day variation in EIA region should be ascribed to enhanced 10-day planetary  
197 wave in lower atmosphere associated with SSW.

198

199 **Acknowledgements:** The GPS data were from the Crustal Movement Observation Network of China (via  
200 e-mail to [yglyang@cma.gov.cn](mailto:yglyang@cma.gov.cn)) and IGS (available at <http://sopac.ucsd.edu>). The GIMs were downloaded  
201 from the site <ftp://cdis.gsfc.nasa.gov>. This research was jointly supported by the National Natural Science  
202 Foundation of China (41464006, 41674157, and 41864006), Guangxi Natural Science Foundation  
203 (2016GXNSFAA380132), and Chinese Meridian Project. We gratefully acknowledge National Center for  
204 Environmental Prediction (NCEP) for providing public access to stratospheric data (available at  
205 <https://www.esrl.noaa.gov/psd/data/reanalysis/>).

206

## 207 **References**

208 Andrews, D. G., Holton, J. R., and Leovy, C. B.: Middle Atmosphere Dynamics, Academic, San Diego,  
209 Calif, 1987.  
210 Andrew, J. D., Vincent, R. A., Murphy, D. J., Tsutsumi, M., Riggin, D. M., and Jarvis, M. J.: The



211 large-scale dynamics of the mesosphere-lower thermosphere during the Southern Hemisphere  
212 stratospheric warming of 2002, *Geophys. Res. Lett.*, 31, L14102, doi:10.1029/2004GL020282, 2004

213 Baldwin, M., Hirooka, T., O'Neill, A., and Yoden, S.: major stratospheric warming in the Southern  
214 Hemisphere in 2002: Dynamical aspects of the ozone hole split, *SPARC Newsl.*, 20, 24-26, 2003.

215 Chang, L. C., Palo, S. E., and Liu, H. -L.: Short-term variation of the s=1 nonmigrating semidiurnal tide  
216 during the 2002 stratospheric sudden warming, *J. Geophys. Res.*, 114, D03109,  
217 doi:10.1029/2008JD010886, 2009.

218 Chau, J. L., Fejer, B. G., and Goncharenko, L. P.: Quiet variability of equatorial  $E \times B$  drift during a  
219 sudden stratospheric warming event. *Geophys. Res. Lett.*, 36,  
220 L05101, <https://doi.org/10.1029/2008GL036785>, 2009.

221 Eswaraiah, S., Kim, Y. H., Lee, J., Ratnam, M. V., and Rao, S. V. B.: Effect of Southern Hemisphere  
222 sudden stratospheric warmings on Antarctica mesospheric tides: First observational study. *J. Geophys.*  
223 *Res. Space Physics*, 123, 2127–2140, <https://doi.org/10.1002/2017JA024839>, 2018.

224 Fejer, B. G., Olson, M. E., Chau, J. L., Stolle, C., Lühr, H., Goncharenko, L. P., Yumoto, K., and  
225 Nagatsuma, T.: Lunar-dependent equatorial ionospheric electrodynamic effects during sudden  
226 stratospheric warmings, *J. Geophys. Res.*, 115, A00G03, doi:10.1029/2010JA015273, 2010.

227 Goncharenko L. P., Chau, J. L., Liu, H. -L., and Coster, A. J.: Unexpected connections between the  
228 stratosphere and ionosphere, *Geophys. Res. Lett.*, 37, L10101, doi:10.1029/2010GL043125, 2010.

229 Gu, S.-Y., Liu, H.-L., Li, T., Dou, X., Wu, Q., and Russell III, J. M.: Observation of the neutral-ion  
230 coupling through 6 day planetary wave, *J. Geophys. Res. Space Physics*, 119, 10,376–10,383,  
231 doi:10.1002/2014JA020530, 2014.

232 Hirota, I., Kuroi, K., and Shiotani, M.: Midwinter warmings in the Southern Hemisphere stratosphere in  
233 1988, *Q. J. R. Meteorol., Soc.*, 116, 929-941, 1990.

234 Hofmann - Wellenhof, B., Lichtenegger, H., and Collins, J.: *GPS—Theory and Practice*, Springer, New  
235 York, 1992.

236 Huang, Y. N., Cheng, K., and Chen, S. W.: On the equatorial anomaly of the ionospheric total electron  
237 content near the northern anomalycrest region, *J. Geophys. Res.*, 94(A10), 13,515–13,525, 1989.

238 Krüger, K., Naujokat, B., and Labitzke, K.: The unusual midwinter warming in the Southern Hemisphere  
239 stratosphere 2002: A comparison to Northern Hemisphere phenomena, *J. Atmos. Sci.*, 62, 603-613,  
240 2005.

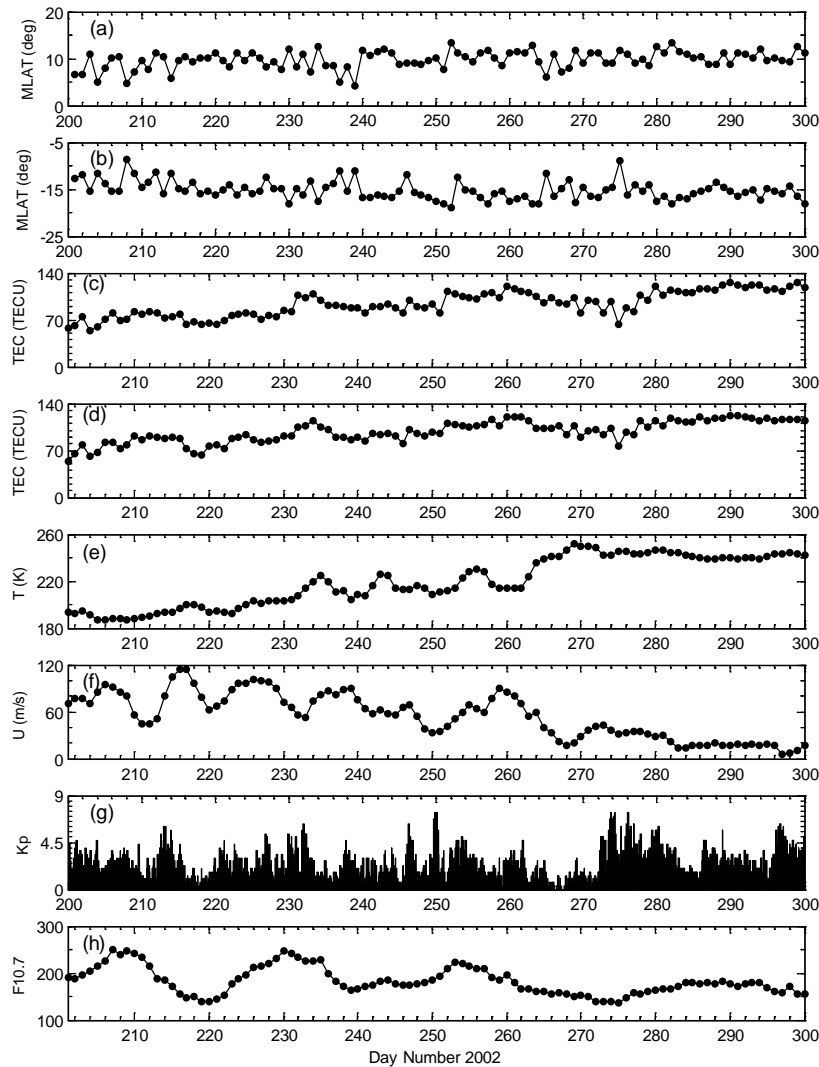




- 241 Lei, J., Thayer, J. P., Forbes, J. M., Wu, Q., She, C., Wan, W., and Wang, W.: Ionosphere response to solar  
242 wind high-speed streams, *Geophys. Res. Lett.*, 35, L19105, doi:10.1029/2008GL035208, 2008.
- 243 Liu, H. -L, Wang, W., Richmond, A. D., and Roble, R. G.: Ionospheric variability due to planetary waves  
244 and tides for solar minimum conditions, *J. Geophys. Res.*, 115, A00G01, doi:10.1029/2009JA015188,  
245 2010.
- 246 Lomb, N. R.: Least-squares frequency analysis of unequally spaced data, *Astrophys.Space Sci.*, 39,  
247 447-462, 1976.
- 248 Mannucci, A. J., Wilson, B. D., Yuan, D. N., Ho, C. M., Lindqwister, U. J., and Runge, T. F.: A global  
249 mapping technique for GPS derived ionospheric total electron content measurements, *Radio Sci.*, 33,  
250 565-582, doi:10.1029/97RS02707, 1998.
- 251 Matsuno, T.: A dynamical model of the stratospheric sudden warming, *J. Atmos. Sci.*, 28, 1479-1494, 1971.
- 252 Mo, X. H., Zhang, D. H., Goncharenko, L. R., Hao, Y. Q., and Xiao, Z.: Quasi-16-day periodic meridional  
253 movement of the equatorial ionization anomaly, *Ann. Geophys.*, 32, 121-131, 2014.
- 254 Mo, X. H., Zhang, D. H., Goncharenko, L. R., Zhang, S. R., Hao, Y. Q., Xiao, Z., Pei, J. Z., Yoshikawa, A.,  
255 Chau, H. D.: Meridional movement of northern and southern equatorial ionization anomaly crests in the  
256 East-Asian sector during 2002–2003 SSW, *Science China Earth Sciences*, 60(4), 776–785, [https://](https://doi.org/10.1007/s11430-016-0096-y)  
257 [doi.org/10.1007/s11430-016-0096-y](https://doi.org/10.1007/s11430-016-0096-y), 2017.
- 258 Mo, X. H., and Zhang, D. H.: Lunar tidal modulation of periodic meridional movement of equatorial  
259 ionization anomaly crest during sudden stratospheric warming, *J. Geophys. Res. Space Physics*, 123,  
260 1488-1499, <https://doi.org/10.1002/2017JA024718>, 2018.
- 261 Olson, M. E., Fejer, B. G., Stolle, C., Lühr, H., and Chau, J. L.: Equatorial ionospheric electrodynamic  
262 perturbations during Southern Hemisphere stratospheric warming events, *J. Geophys. Res. Space*  
263 *Physics*, 118, 1190-1195, doi:10.1002/jgra.50142, 2013.
- 264 Palo S. E., Forbes, J. M., Zhang, X., Russell III, J. M., Mertens, C. J., Mlynczak, M. G., Burns, G. B., Espy,  
265 P. J., and Kawahara, T. D.: Planetary wave coupling from the stratosphere to the thermosphere during the  
266 2002 Southern Hemisphere pre-stratwam period, *Geophys. Res. Lett.*, 32, L23809,  
267 doi:10.1029/2005GL024298, 2005.
- 268 Park, J., Lühr, H., Kunze, M., Fejer, B. G., and Min, K. W.: Effect of sudden stratospheric warming on  
269 lunar tidal modulation of the equatorial electrojet, *J. Geophys. Res.*, 117, A03306,  
270 doi:10.1029/2011JA017351, 2012.

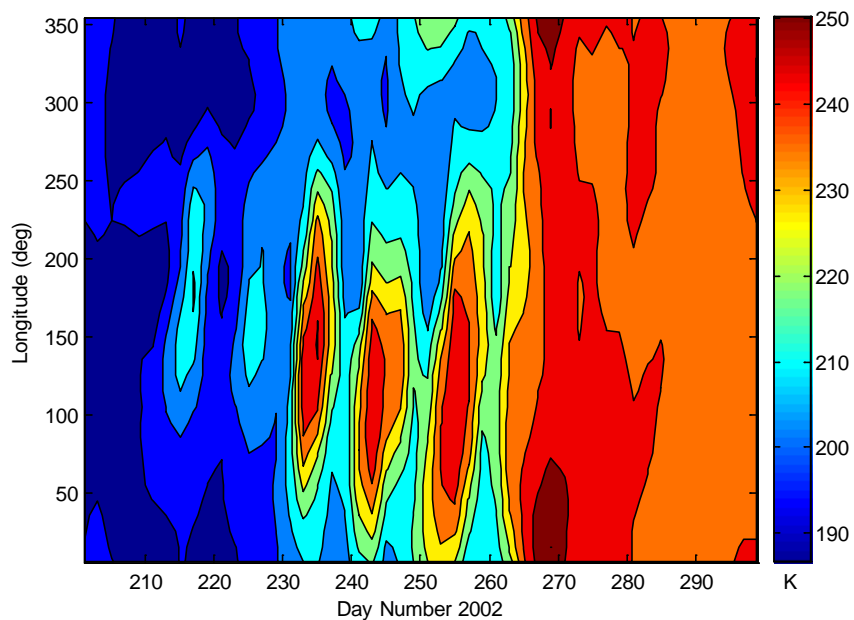


- 271 Pedatella, N. M., and Forbes, J. M.: Modulation of the equatorial F-region by the quasi-16 day planetary  
272 wave, *Geophys. Res. Lett.*, 34, L09105, doi:10.1029/2009GL037809, 2009.
- 273 Pedatella, N. M., and Forbes, J. M.: Evidence for stratosphere sudden warming-ionosphere coupling due to  
274 vertically propagating tides, *Geophys. Res. Lett.*, 37, L11104, doi:10.1029/2010GL043560, 2010.
- 275 Pedatella, N. M.: Observations and simulations of the ionospheric lunar tide: Seasonal variability, *J.*  
276 *Geophys. Res. Space Physics*, 119, 5800-5806, doi:10.1002/2014JA020189, 2014.
- 277 Scargle, J. D.: Studies in astronomical time series analysis. II. Statistical aspects of spectral analysis of  
278 unevenly spaced data, *Astrophys. J.*, 263, 835-853, 1982.
- 279 Scherhag, R.: Die explosionsartigen Stratosphärenwärmungen des Spätwinters 1952, *Ber. Dtsch*  
280 *Wetterdienstes USZone*, 6, 51-63, 1952.
- 281 Stening, R. J.: Lunar tide in the equatorial electrojet in relation to stratospheric warmings, *J. Geophys. Res.*,  
282 116, A12315, doi:10.1029/2011JA017047, 2011.
- 283 Ushimaru, S., and Tanaka, H.: A numerical study of the interaction between stationary Rossby waves and  
284 eastward-traveling waves in the Southern Hemisphere stratosphere, *J. Atmos., Sci.*, 49, 1354-1373,  
285 1992.
- 286 Varotsos, C.: The Southern Hemisphere ozone hole split in 2002, *Environ. Sci. Pollut. Res.*, 9, 375-376,  
287 2002.
- 288 Venkat Ratnam, M., Tsuda, T., Jacobi, C., and Aoyama, Y.: Enhancement of gravity wave activity observed  
289 during a major Southern Hemisphere stratospheric warming by CHAMP/GPS measurements, *Geophys.*  
290 *Res. Lett.*, 31, L16101, doi:10.1029/2004GL019789, 2004.
- 291 Vineeth, C., Pant, T. K., Devasia, C. V., and Sridharan, R.: Atmosphere-ionosphere coupling observed over  
292 the dip equatorial MLTI region through the quasi 16-day wave. *Geophys. Res. Lett.*, 34,  
293 L12102, <https://doi.org/10.1029/2007GL030010>, 2007.
- 294 Yeh, K. C., Franke, S. J., Andreeva, E. S., and Kunitsyn, V. E.: An investigation of motions of the  
295 equatorial anomaly crest, *Geophys. Res. Lett.*, 28(24), 4517-4520, doi:10.1029/2001GL013897, 2001.
- 296  
297  
298  
299



300

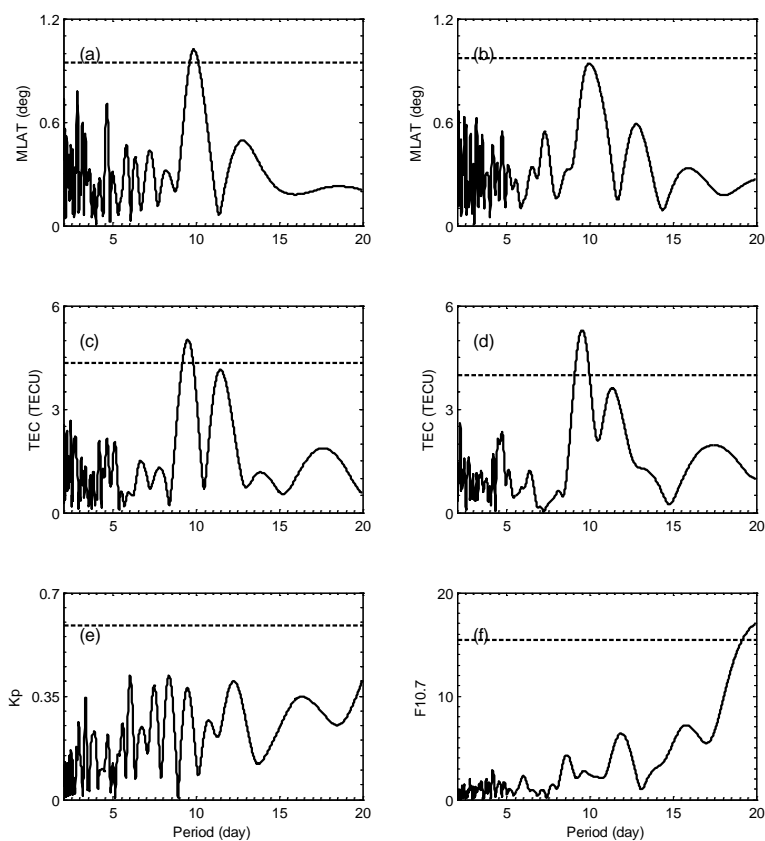
301 **Figure 1.** The magnetic latitude (MLAT ) location of (a) northern and (b) southern equatorial ionization  
302 anomaly (EIA) crest; The TEC of (c) northern and (d) southern EIA crest; the (e) polar stratospheric  
303 temperature (at 90°S, 10hPa) and (f) zonal wind (at 60°S, 10hPa) from National Centers for Environment  
304 Prediction; the (g) Geomagnetic activity index, Kp and (h) solar flux index F10.7 during the period from  
305 July 21, 2002 to October 18, 2002.



306

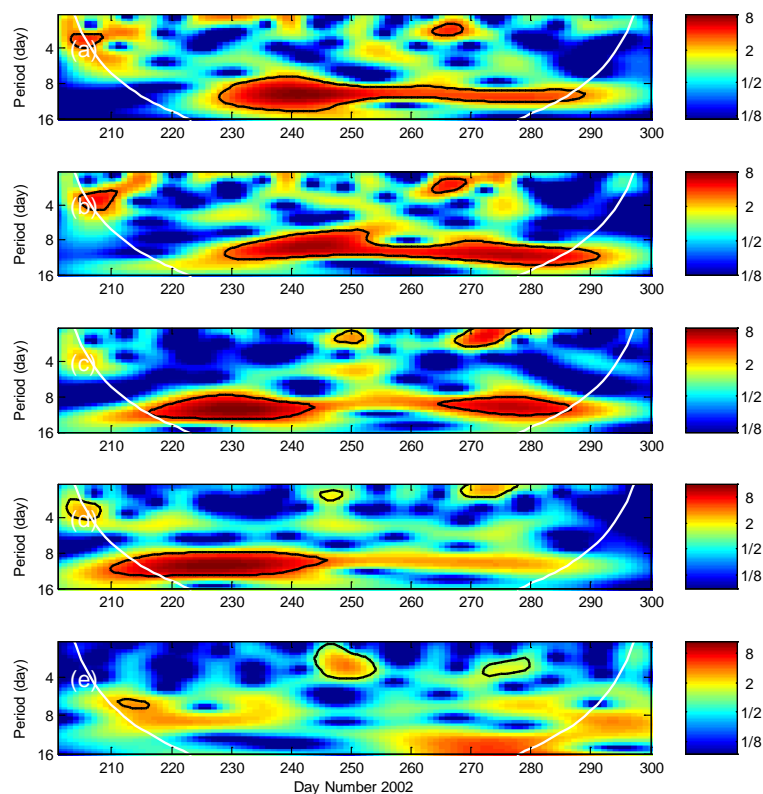
307 **Figure 2.** The contour map of polar stratospheric temperature (80°S, 10hPa) obtained from NCEP during

308 the same period as in Figure 1.



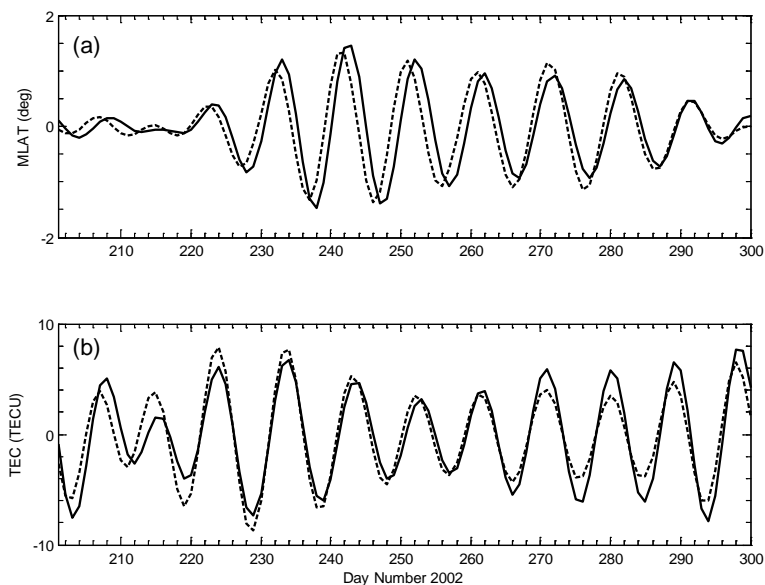
309

310 **Figure 3.** Lomb-Scargle periodograms of the MLAT location of (a) northern and (b) southern EIA crest, the  
311 TEC of (c) northern and (d) southern EIA crest, (e) Kp index and (f) F10.7 during the same period as in  
312 Figure 1.



313

314 **Figure 4.** The wavelet power spectra of the MLAT location of (a) northern and (b) southern EIA crest, the  
315 TEC of (c) northern and (d) southern EIA crest, (e) Kp index during the same period as in Figure 1. The  
316 white line in each panel represents the cone of influence of the wavelet analysis.



317

318 **Figure 5.** The band-pass filter results of the (a) MLAT location of (solid line) northern and (dash-dotted  
319 line) southern EIA crest, the (b) TEC of (solid line) northern and (dash-dotted line) southern EIA crest  
320 during the same period as in Figure 1.